distance in each case). The net nitrogen charges obtained from the calculations are given in Table III. Structure I is indicated by these calculations; indeed structure III would be predicted to show only one peak, for the two different nitrogens are predicted to have approximately the same charge. Finally it can be seen in Figures 2 and 3 that the points representing structure I do fit the correlation lines. Recently the oxyhyponitrite ion has been shown by asymmetric ^{15}N-labeling to have two structurally different nitrogen atoms.[22]

(22) D. N. Hendrickson and W. L. Jolly, *Inorg. Chem.*, **8**, 693 (1969).

CONTRIBUTION FROM THE NOYES CHEMICAL LABORATORY,
UNIVERSITY OF ILLINOIS, URBANA, ILLINOIS 61801

Zeeman Studies Including the Molecular g Values, Magnetic Susceptibilities, and Molecular Quadrupole Moments in Phosphorus and Nitrogen Trifluorides and Phosphoryl, Thionyl, and Sulfuryl Fluorides

BY R. G. STONE, J. M. POCHAN, AND W. H. FLYGARE

The high-field and first- and second-order Zeeman effect has been observed in phosphorus trifluoride (PF_3), nitrogen trifluoride (NF_3), phosphoryl fluoride (POF_3), thionyl fluoride (SOF_2), and sulfuryl fluoride (SO_2FO_2). For PF_3 the g values perpendicular and parallel to the molecular symmetry axis are $|g_\perp| = 0.0659 \pm 0.0003$ and $|g_\parallel| = 0.0815 \pm 0.0020$. The average magnetic susceptibility anisotropy is $\chi_\perp - \chi_\parallel = (1.32 \pm 0.20) \times 10^{-6}$ erg/G^2 mol. Using an appropriate choice for the g-value signs gives the quadrupole moment of $Q_\parallel = +(24.1 \pm 3.1) \times 10^{-26}$ esu cm^2. The paramagnetic susceptibilities are $\chi^p_\perp = 147.9 \pm 1.0$ and $\chi^p_\parallel = 259.6 \pm 1.0$ in units of 10^{-6} erg/G^2 mol. The anisotropy in the second moments of the electronic charge distributions is $\langle\parallel^2\rangle - \langle\perp^2\rangle = -(26.6 \pm 0.4) \times 10^{-6}$ cm^2. For POF_3, the values for the perpendicular g value and the magnetic susceptibility anisotropy are $|g_\perp| = 0.0440 \pm 0.0005$ and $\chi_\perp - \chi_\parallel = (1.78 \pm 0.18) \times 10^{-6}$ erg/G^2 mol. Assuming $g_\parallel = -0.0815$ as in PF_3 and the negative sign for $g_\perp$ gives the molecular quadrupole moment of $Q_\parallel = (20.4) \times 10^{-26}$ esu cm^2. The paramagnetic susceptibilities are $\chi^p_\perp = 251.4 \pm 1.0$ and $\chi^p_\parallel = 245.9 \pm 1.0$ in units of 10^{-6} erg/G^2 mol. The anisotropy in the second moment of the electronic charge distribution is $\langle\parallel^2\rangle - \langle\perp^2\rangle = -(1.7 \pm 0.4) \times 10^{-16}$ cm^2. For NF_3 the g value perpendicular to the molecular symmetry axis was measured as $g_\perp = -(0.060 \pm 0.001)$. The magnetic susceptibility anisotropy was measured as $\chi_\perp - \chi_\parallel = -(3.0 \pm 1.5) \times 10^{-6}$ erg/G^2 mol. For SOF_2 the g values in the principal inertial axis system are $|g_{aa}| = 0.0802 \pm 0.0070$, $|g_{bb}| = 0.0856 \pm 0.0051$, and $|g_{cc}| = 0.1093 \pm 0.0038$. The magnetic susceptibility anisotropies are $2\chi_{aa} - \chi_{bb} - \chi_{cc} = (0.7 \pm 1.6) \times 10^{-6}$ erg/G^2 mol and $2\chi_{bb} - \chi_{cc} - \chi_{aa} = -(1.5 \pm 2.0) \times 10^{-6}$ erg/G^2 mol. Using the negative signs for the g values gives the molecular quadrupole moments of $Q_{aa} = -12.5 \pm 4.5$, $Q_{bb} = -17.0 \pm 4.5$, and $Q_{cc} = 29.5 \pm 5.6$, all in units of 10^{-26} esu cm^2. The diagonal elements in the paramagnetic susceptibility tensor are $\chi^p_{aa} = 125.0 \pm 2.0$, $\chi^p_{bb} = 156.9 \pm 2.0$, and $\chi^p_{cc} = 251.0 \pm 2.0$, all in units of 10^{-6} erg/G^2 mol. The anisotropies in the second moment of the electronic charge distribution are $\langle a^2\rangle - \langle b^2\rangle = (7.7 \pm 1.0) \times 10^{-16}$ cm^2, $\langle b^2\rangle - \langle c^2\rangle = (22.0 \pm 1.2) \times 10^{-16}$ cm^2, and $\langle c^2\rangle - \langle a^2\rangle = -(29.7 \pm 1.3) \times 10^{-16}$ cm^2. For SO_2F_2 the g values in the principal inertial axis system are $|g_{aa}| = 0.0447 \pm 0.0068$, $|g_{bb}| = 0.0456 \pm 0.0015$, and $|g_{cc}| = 0.0565 \pm 0.0009$. The magnetic susceptiblity anisotropies are $2\chi_{aa} - \chi_{bb} - \chi_{cc} = -12.6 \pm 2.6$ and $2\chi_{bb} - \chi_{cc} - \chi_{aa} = 13.2 \pm 3.5$, both in units of 10^{-6} erg/G^2 mol. Using the negative g-value signs gives the molecular quadrupole moments of $Q_{aa} = 3.9 \pm 5.3$, $Q_{bb} = -9.7 \pm 4.6$, and $Q_{cc} = 5.9 \pm 5.9$, all in units of 10^{-26} esu cm^2. The diagonal elements of the paramagnetic susceptibility tensor are $\chi^p_{aa} = 221.6 \pm 3.1$, $\chi^p_{bb} = 227.4 \pm 1.0$, and $\chi^p_{cc} = 226.4 \pm 1.0$, all in units of 10^{-6} erg/G^2 mol. The anisotropies in the second moment of the electronic charge distribution are $\langle a^2\rangle - \langle b^2\rangle = -0.6 \pm 1.4$, $\langle b^2\rangle - \langle c^2\rangle = 0.8 \pm 1.1$, and $\langle c^2\rangle - \langle a^2\rangle = -0.2 \pm 1.5$, all in units of 10^{-16} cm^2.

I. Introduction

Phosphorus trifluoride (PF_3), nitrogen trifluoride (NF_3), phosphoryl fluoride (OPF_3), thionyl fluoride (SOF_2) and sulfuryl fluoride (SO_2F_2) are all similar inorganic molecules. A comparison of the charge distribution, obtained from the molecular quadrupole moments, would be of considerable interest. Microwave spectroscopy has recently been developed as an effective method of determining molecular quadrupole moments and electronic charge anisotropies.[1,2] This method, which has been applied to several molecules,[3] involves the measurement of both the *first-* and *second-*order magnetic field effects. The first-order Zeeman effect gives the molecular magnetic rotational moments or molecular g values. The second-order Zeeman effect gives the anisotropies in the magnetic susceptibilities. The combination of the first- and second-

(1) W. Hüttner and W. H. Flygare, *J. Chem. Phys.*, **47**, 4137 (1967).
(2) W. Hüttner, M. K. Lo, and W. H. Flygare, *ibid.*, **48**, 1206 (1968).

(3) Summaries, references, and discussions of fluorobenzene, thiophene, furan, cyclopropene, ethylene oxide, ethylene sulfide, acetaldehyde, formic acid, formaldehyde, OCS, NNO, HC≡CF, ketene, water, and ammonia are given by D. H. Sutter and W. H. Flygare, *Mol. Phys.*, **16**, 153 (1969), and *J. Am. Chem. Soc.*, **91**, 4063 (1969); S. G. Kukolich and W. H. Flygare, *Mol. Phys.*, **17**, 127 (1969), and *J. Am. Chem. Soc.*, **91**, 2433 (1969); R. L. Shoemaker, W. Hüttner, and W. H. Flygare, *J. Chem. Phys.*, **50**, 2414 (1969). See also references 2, 4, and 5 of this paper.

order Zeeman effects leads to an experimental determination of the molecular quadrupole moments.[2]

In this paper we have measured the molecular g values and magnetic susceptibility anisotropies in PF_3, NF_3, OPF_3, SOF_2, and SO_2F_2. We also give the resultant molecular quadrupole moments which give the second moments of the electronic charge distributions.

II. Theory

The rotational energy levels for a molecule in the presence of a magnetic field are given in eq 28 of Hüttner and Flygare.[1] In the absence of nuclear spin, this equation reduces to

$$E(J, M_J) = -\frac{1}{2}\chi H^2 - \mu_0 \frac{M_J H}{J(J+1)}\sum_g g_{gg}\langle P_a{}^2\rangle -$$
$$H^2\left[\frac{3M_J{}^2 - J(J+1)}{(2J-1)(2J+3)}\right]\left[\frac{1}{J(J+1)}\right]\sum_g(\chi_{gg} - \chi)\langle P_g{}^2\rangle$$
$$(1)$$

where $\chi = \frac{1}{3}(\chi_{aa} + \chi_{bb} + \chi_{cc})$ is the average bulk magnetic susceptibility with χ_{aa}, χ_{bb}, and χ_{cc} being the components along the principal inertial axes in the molecule. H is the external magnetic field, μ_0 is the nuclear magneton, J and M_J are the rotational quantum numbers, and $\langle P_g{}^2\rangle$ is the average value of the squared rotational angular momentum (in units of $\hbar^2$) along the gth principal inertial axis. $\langle P_a{}^2\rangle$, $\langle P_b{}^2\rangle$, and $\langle P_c{}^2\rangle$ are readily evaluated from the assigned rotational spectra. Since we are observing differences in energy levels, the $-\frac{1}{2}\chi H^2$ term will cancel. The magnetic anisotropy components are

$$\chi_{aa} - \chi = \frac{1}{3}(2\chi_{aa} - \chi_{bb} - \chi_{cc})$$
$$\chi_{bb} - \chi = \frac{1}{3}(-\chi_{aa} + 2\chi_{bb} - \chi_{cc}) \qquad (2)$$
$$\chi_{cc} - \chi = \frac{1}{3}(-\chi_{aa} - \chi_{bb} + 2\chi_{cc})$$

Only two of these equations are independent. Our least-squares data analysis program for asymmetric rotors has been written to give the values of $2\chi_{aa} - \chi_{bb} - \chi_{cc}$ and $2\chi_{bb} - \chi_{aa} - \chi_{cc}$.[2,4,5] The third anisotropy component is the negative sum of the first two as the trace of the $\chi_{gg} - \chi$ tensor is zero. g_{gg} is the molecular g value along the gth principal inertial axis given by

$$g_{xx} = \frac{M_p}{I_{xx}m}\left[m\sum_n Z_n(r_n{}^2 - x_n{}^2) + 2\sum_{k>0}\frac{|\langle 0|L_x|k\rangle|^2}{E_0 - E_k}\right] \qquad (3)$$

where M_p and m are the proton and electron masses, I_{xx} is the principal moment of inertia, Z_n is the atomic number of the nth nucleus at distance r_n and projection x_n from the molecular center of mass, L_x is the electronic angular momentum operator, and the sum is over all

excited electronic states $|k\rangle$ with energy E_k. The magnetic susceptibility terms, χ_{xx}, are defined later.

In summary, by computing $\langle P_a{}^2\rangle$, $\langle P_b{}^2\rangle$, and $\langle P_c{}^2\rangle$ by standard methods, in a general asymmetric top, the first- and second-order Zeeman effects can give the absolute values of three g values (g_{aa}, g_{bb}, and g_{cc}) and the values of two independent magnetic susceptibility parameters ($(2\chi_{aa} - \chi_{bb} - \chi_{cc})$ and $(2\chi_{bb} - \chi_{cc} - \chi_{cc})$). SOF_2 and SO_2F_2 in the present study are asymmetric tops.

In the case of symmetric-top molecules like the PF_3, NF_3, and OPF_3

$$\langle P_a{}^2\rangle = \langle P_b{}^2\rangle = \frac{1}{2}[J(J+1) - K^2] \qquad (4)$$

and

$$\langle P_c{}^2\rangle = K^2 \qquad (5)$$

Substituting eq 4 and 5 into eq 1 gives the rotational Zeeman energy for a symmetric top as shown by Shoemaker and Flygare.[6] K is the projection of J on the molecular symmetry axis. $g_\perp$ and $\chi_\perp$ are the g value and

$$E(J, M_J) = -\mu_0 M_J H\left[g_\perp + (g_{||} - g_\perp)\frac{K^2}{J(J+1)}\right] -$$
$$\frac{H^2}{3}\left[\frac{3M_J{}^2 - J(J+1)}{(2J-1)(2J+3)}\right]\left[(\chi_\perp - \chi_{||}) - \frac{3K^2}{J(J+1)}(\chi_\perp - \chi_{||})\right] \qquad (6)$$

total magnetic susceptibility component, respectively, along the axes perpendicular to the C_3 symmetry axis in the symmetric top. $g_{||}$ and $\chi_{||}$ are the corresponding components parallel to the symmetry axis. In the symmetric-top expression in eq 6, it is evident that only three parameters can be measured, namely, the two g values ($g_\perp$ and $g_{||}$) and the single magnetic susceptibility anisotropy ($\chi_\perp - \chi_{||}$).

The $K = 0$ Zeeman energy for a symmetric top (from eq 6) is identical with the expression for a linear molecule. Substituting $K = 0$ into eq 6 gives

$$E(J, M_J) = -H\mu_0 M_J g_\perp - \frac{H^2}{3} \times$$
$$\left[\frac{3M_J{}^2 - J(J+1)}{(2J-1)(2J+3)}\right](\chi_\perp - \chi_{||}) \qquad (7)$$

In this case, only two Zeeman parameters can be measured.

The $^{14}NF_3$ case is more complicated due to the large ^{14}N nuclear quadrupole coupling. This additional complication will be discussed in the following section on NF_3.

After extracting the molecular g values and magnetic susceptibility anisotropies, the molecular quadrupole moments are directly obtained. The general expression

(4) W. Hüttner and W. H. Flygare, *J. Chem. Phys.*, **50**, 2863 (1969).
(5) D. H. Sutter, W. Hüttner, and W. H. Flygare, *ibid.*, **50**, 2869 (1969).

(6) R. L. Shoemaker and W. H. Flygare, *J. Am. Chem. Soc.*, **91**, 5417 (1969).

for an asymmetric top is given by Hüttner, Lo, and Flygare[2] as

$$Q_{cc} = \frac{|e|}{2}\sum_n Z_n(3z_n^2 - r_n^2) - \frac{|e|}{2}\langle 0 \mid \sum_i (3z_i^2 - r_i^2) \mid 0 \rangle$$

$$= \frac{|e|}{2}\sum_n Z_n(3z_n^2 - r_n^2) - \frac{|e|}{2}[3\langle z^2 \rangle - \langle r^2 \rangle]$$

$$= \frac{\hbar|e|}{8\pi M}\left[\frac{2g_{cc}}{C} - \frac{g_{aa}}{A} - \frac{g_{bb}}{B}\right] - \frac{2mc^2}{|e|N} \times$$

$$(2\chi_{cc} - \chi_{aa} - \chi_{bb}) \quad (8)$$

where $|e|$ is the electronic charge, M is the proton mass, N is Avogadro's number, and A, B, and C are the rotational constants. Z_n is the atomic number of the nth nucleus, and a_n and b_n are nuclear coordinates in the principal inertial axis system (see Figure 1). Similar expressions for Q_{aa} and Q_{bb} are obtained by cyclic permutations. The second moments of the electronic charge distribution are defined as

$$\langle a^2 \rangle = \langle 0 \mid \sum_i a_i^2 \mid 0 \rangle$$

$$\langle b^2 \rangle = \langle 0 \mid \sum_i b_i^2 \mid 0 \rangle \quad (9)$$

$$\langle c^2 \rangle = \langle 0 \mid \sum_i c_i^2 \mid 0 \rangle$$

where a_i, b_i, and c_i are the components of the position vector of the ith electron along the gth inertial axis and $\langle 0 \mid \mid 0 \rangle$ indicates an expectation value in the ground electronic state.

In the case of a symmetric top eq 8 can be simplified. If $b = c$ and a is the symmetry axis, eq 7 reduces to

$$Q_{aa} = \frac{\hbar|e|}{4\pi M}\left[\frac{2g_{aa}}{A} - \frac{2g_{bb}}{B}\right] - \frac{4mc^2}{|e|N}[2\chi_{aa} - 2\chi_{bb}] =$$

$$-2Q_{bb} = -2Q_{cc}$$

$$Q_{||} = -\frac{\hbar e}{4\pi M}\left[\frac{g_{||}}{G_{||}} - \frac{g_\perp}{G_\perp}\right] - \frac{4mc^2}{|e|N}(\chi_{||} - \chi_\perp) = -2Q_\perp$$

$$(10)$$

The anisotropies in the second moment of the electronic charge distribution can be related to the known molecular structure and the Zeeman constants. The appropriate expression is

$$\langle b^2 \rangle - \langle a^2 \rangle = \sum_n Z_n(b_n^2 - a_n^2) + \frac{\hbar}{4\pi M}\left(\frac{g_{bb}}{B} - \frac{g_{aa}}{A}\right) +$$

$$\frac{4mc^2}{3e^2N}[(2\chi_{bb} - \chi_{aa} - \chi_{cc}) - (2\chi_{aa} - \chi_{bb} - \chi_{cc})] \quad (11)$$

Similar expressions for $\langle c^2 \rangle - \langle b^2 \rangle$ and $\langle a^2 \rangle - \langle c^2 \rangle$ are readily obtained. The molecular structures in the present study necessary to extract a_n^2, b_n^2, and c_n^2 are shown in Figure 1.

The diagonal elements in the paramagnetic susceptibility tensor (χ^P_{zz}) can also be obtained from the molecu-
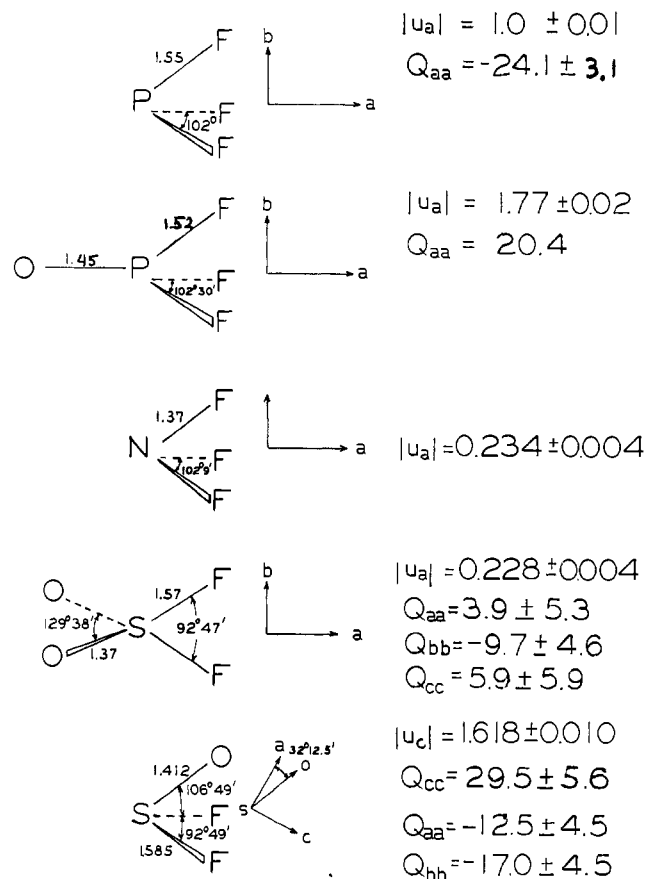

Figure 1.—The molecular structures and orientation of the principal inertial axes in the molecules studied here. Also listed are the electric dipole and quadrupole moments.

lar structures and the molecular g values. The appropriate equation is

$$\chi^P_{aa} = -\frac{e^2N}{2m^2c^2}\sum_k \frac{\langle 0 \mid L_a \mid k \rangle|^2}{E_0 - E_k} = -\frac{e^2N}{2mc^2} \times$$

$$\left[\frac{\hbar g_{aa}}{8\pi G_{aa}M} - \frac{1}{2}\sum_n Z_n(b_n^2 + c_n^2)\right] \quad (12)$$

The total magnetic susceptibility, χ_{zz}, along any axis is a sum of diamagnetic, χ^d_{zz}, and paramagnetic, χ^P_{zz}, components defined by

$$\chi_{aa} = \chi^P_{aa} + \chi^d_{aa}$$

$$\chi^d_{aa} = -\frac{e^2N}{4mc^2}\langle 0 \mid \sum_i (b_i^2 + c_i^2) \mid 0 \rangle \quad (13)$$

If the bulk magnetic susceptibility, χ, is known then the individual elements of the χ_{zz}, χ^d_{zz}, and $\langle x^2 \rangle$ tensors can be obtained by straightforward manipulations of the above equations. For instance

$$\langle x^2 \rangle = -\frac{2mc^2}{Ne^2}[(\chi_{yy} + \chi_{zz} - \chi_{xx}) - (\chi^P_{yy} + \chi^P_{zz} - \chi^P_{xx})]$$

$$(14)$$

III.   Experimental Work and Extraction of the Molecular Parameters

The microwave spectrograph and high-field electromagnet used here has been described before.[7]   Briefly, the microwave spectrograph is a 2.0–40.0-GHz phase-stabilized system with slow, stable sweep facilities.   A 5.0–100.0-kHz Stark modulation is used in 6-ft cells of either X-band or C-band cells.   The magnet is a typical H-frame system with magnetic fields over a full 6 ft with fields up to 30,000 G.

The zero-field microwave spectra of each of the molecules studied here is well known; PF_3,[8] POF_3,[9] NF_3,[10] SOF_2,[11] and SO_2F_2.[12]   The rotational constants in these references are used to compute the values of $\langle P_a^2 \rangle$, $\langle P_b^2 \rangle$, and $\langle P_c^2 \rangle$ in the SOF_2 and SO_2F_2 asymmetric-top molecules.   The molecular structures used in the present analysis are given in the above references and are also listed in Figure 1.

The following sections give specific details of the experiments and data analysis of each of the molecules studied here.

PF_3.—The $J = 0 \rightarrow 1$, $\Delta M = 1$, $K = 0$ doublet was observed several times at a field of 25,386 G (see Figure 2 for one of the traces), and was split by 2554 ± 10 kHz.   The quoted splitting is a statistical average of the several sweeps.   Equation 7 shows that the splitting leads directly to $g_\perp$ as the $(\chi_\perp - \chi_{||})$ term drops out.   From this datum the absolute value of the resultant $g_\perp$ is

$$|g_\perp| = 0.0659 \pm 0.0003 \tag{15}$$

The most probable sign of $g_\perp$ will be determined below.

The $J = 0 \rightarrow 1$, $\Delta M = 0$, $K = 0$ singlet was observed several times at a field of 28,982 G and was shifted in frequency by +37 ± 5 kHz.   This observed shift is an average of the several sweeps.   The $(\chi_\perp - \chi_{||})$ term in eq 7 for the $J = 0 \rightarrow 1$, $\Delta M = 0$ transition is twice the value for the $J = 0 \rightarrow 1$, $\Delta M = \pm 1$ doublet.   Since this shift is larger and more accurate than the shift obtained from the $J = 0 \rightarrow 1$, $\Delta M = \pm 1$ transitions, it was used to calculate $\chi_\perp - \chi_{||}$.   The resultant value is

$$\chi_\perp - \chi_{||} = (1.32 \pm 0.18) \times 10^{-6} \text{ erg/G}^2 \text{ mol} \tag{16}$$

The $J = 1 \rightarrow 2$, $K = 1$, $\Delta M = \pm 1$ transitions were observed at a field of 25,055 G (see Figure 3) in order to obtain $g_{||}$.   Equation 6 describes this $K = 1$, $J = 1 \rightarrow J = 2$, $\Delta M = \pm 1$ spectrum.   There are six expected components with the energies and relative intensities shown in Table I.

Table I

Transition	Energy	Rel intens
$M_J = 0 \rightarrow 1$	$-\dfrac{\mu_0 H}{6}(5g_\perp + g_{||}) + \dfrac{19H^2}{210}(\chi_\perp - \chi_{||})$	6
$M_J = 0 \rightarrow -1$	$+\dfrac{\mu_0 H}{6}(5g_\perp + g_{||}) + \dfrac{19H^2}{210}(\chi_\perp - \chi_{||})$	6
$M_J = 1 \rightarrow 2$	$-\dfrac{\mu_0 H}{6}(7g_\perp - g_{||}) - \dfrac{17H^2}{210}(\chi_\perp - \chi_{||})$	12
$M_J = 1 \rightarrow 0$	$+\dfrac{\mu_0 H}{2}(g_\perp + g_{||}) + \dfrac{H^2}{70}(\chi_\perp - \chi_{||})$	2
$M_J = -1 \rightarrow -2$	$+\dfrac{\mu_0 H}{6}(7g_\perp - g_{||}) - \dfrac{17H^2}{210}(\chi_\perp - \chi_{||})$	12
$M_J = -1 \rightarrow 0$	$-\dfrac{\mu_0 H}{2}(g_\perp + g_{||}) + \dfrac{H^2}{70}(\chi_\perp - \chi_{||})$	2

(7) W. H. Flygare, W. Hüttner, R. L. Shoemaker, and P. D. Foster, *J. Chem. Phys.*, **50**, 1714 (1969).

(8) O. R. Gilliam, H. D. Edwards, and W. Gordy, *Phys. Rev.*, **75**, 1014 (1949).

(9) Q. Williams, J. Sheridan, and W. Gordy, *J. Chem. Phys.*, **20**, 164 (1952).

(10) D. R. Lide, D. E. Mann, and R. M. Fritstrom, *ibid.*, **26**, 734 (1957).

(11) J. Sheridan and W. Gordy, *Phys. Rev.*, **79**, 513 (1950).

(12) R. C. Ferguson, *J. Am. Chem. Soc.*, **76**, 850 (1954).

The $J = 1 \rightarrow J = 2$, $\Delta M = \pm 1$, $K = 1$ spectrum in PF_3 shown in Figure 2 is a doublet with a strong Stark effect near ν_0.   This intense Stark effect was observed previously in the same transition in $CH_3C\equiv CH$ and is described in detail by Shoemaker and Flygare (see next section on OPF_3).[6]   The Stark effect is not of interest here.

In order to interpret the doublet in Figure 2, we first assumed that the doublet was caused entirely by the two most intense components in the above six components.   The average splitting for several observed transitions was 2418 ± 40 kHz.   With the use of the $M_J = 1 \rightarrow 2$ and $M_J = -1 \rightarrow -2$ assignment above, a relation between $g_\perp$ and $g_{||}$ was obtained (eq 17).   Since

$$\frac{\mu_0 H}{3} |(7g_\perp - g_{||})| = 2418 + 40 \text{ kHz} \tag{17}$$

only the absolute value of $g_\perp$ was known, four sets of values were obtained: for $g_\perp = +0.0659$

$$g_{||} = 0.0815 \pm 0.002 \text{ and } 0.8411 \pm 0.002 \tag{18}$$

and for $g_\perp = -0.0659$

$$g_{||} = -0.0815 \pm 0.002 \text{ and } -0.8411 \pm 0.002 \tag{19}$$

Using Table I and eq 15 and 16 we can now compute the six-line spectra which should appear in Figure 3 for either choice for the signs of the g values.   The results are listed in Table II.   The markers in Figure 3 are every 100 kHz.   Therefore, the spectra with $|g_{||}| = 0.8411$ would have resolved into the six components.   The unresolved spectrum observed as shown in Figure 3 is predicted on the basis of $|g_{||}| = 0.0815$ and the approximation of using the strong components to give the g values is shown by Table II to be sound.   On the basis of this analysis we will exclude the g-value combinations with $|g_{||}| = 0.8411$.

Table II

Calculated $\Delta M = \pm 1$ Transition Splittings from ν_0 (in kHz) in the $J = 1 \rightarrow J = 2$, $K = 1$ Transition in PF_3 as Shown in Figure 3 at a Field of 25,055 G[a]

$J = 1 \rightarrow J = 2$ $M \rightarrow M$	Rel intens	$g_\perp = \pm 0.0659$ $g_{||} = \pm 0.0815$	$g_\perp = \pm 0.0659$ $g_{||} = \pm 0.8411$
$-1 \rightarrow 0$	2	-1405 (1411)	8664 (8664)
$0 \rightarrow 1$	6	-1289 (1327)	3745 (3745)
$1 \rightarrow 2$	12	-1226 (1191)	-1226 (-1226)
$-1 \rightarrow -2$	12	1191 (-1226)	1191 (1191)
$0 \rightarrow -1$	6	1327 (-1289)	-3707 (-3707)
$1 \rightarrow 0$	2	1411 (-1405)	-8658 (-8658)

[a] The results are given for both positive and negative values for $g_\perp$ and $g_{||}$ as discussed in eq 18 and 19.   Values for the negative g values are in parentheses.   All frequencies are in kilohertz.

The molecular quadrupole moments in PF_3 are obtained from eq 10 and the values of $g_\perp$, $g_{||}$, and $(\chi_\perp - \chi_{||})$ which are assigned in this section.   The results for both choices for the signs of $g_\perp$ and $g_{||}$ are (in units of 10^{-26} esu cm^2) given in eq 20 and 21.

$g_\perp = -0.0659$ and $g_{||} = -0.0815$
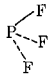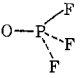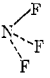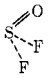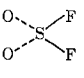
$$Q_{||} = +24.1 \pm 3.1 \tag{20}$$

$g_\perp = +0.0659$ and $g_{||} = +0.0815$

$$Q_{||} = -21.1 \pm 3.1 \tag{21}$$

The assignment of the correct signs for the g values on the basis of the molecular quadrupole moments is not straightforward.   However, the structure of PF_3 as listed in Figure 1 indicates that the distance of the fluorine atoms from the phosphorus atom along the symmetry axis is much less than their distance perpendicular to the symmetry axis.   The molecule is an oblate symmetric top with highly electronegative fluorine atoms at a large distance from the symmetry axis.   The quadrupole moments perpendicular to the symmetry axis would most probably be negative and $Q_{||}$

TABLE III

MOLECULAR ZEEMAN PARAMETERS IN PF_3, OPF_3, NF_3, SOF_2, AND SO_2F_2[a]

	PF_3	OPF_3	NF_3	SOF_2	SO_2F_2
$|g_{xx}|$	0.0659 ± 0.0003	0.0440 ± 0.0005	-0.060 ± 0.001^d	0.0856 ± 0.0051	0.0565 ± 0.001
$|g_{yy}|$	0.0659 ± 0.0003	0.0440 ± 0.0005	-0.060 ± 0.001^d	0.0802 ± 0.0070	0.0456 ± 0.002
$|g_{zz}|$	0.0815 ± 0.0002	0.0815^b		0.1093 ± 0.0038	0.0447 ± 0.007
$2\chi_{zz} - \chi_{xx} - \chi_{yy}$	-2.64 ± 0.36	-3.56 ± 0.36	6.0 ± 3.0	0.8 ± 2.0	-12.6 ± 2.6
$2\chi_{xx} - \chi_{zz} - \chi_{yy}$	$+1.32 \pm 0.18$	$+1.78 \pm 0.18$	-3.0 ± 1.5	-1.5 ± 2.0	-0.6 ± 2.6
Q_{xx}	-12.05 ± 3.1	-10.25^c		12.5 ± 4.5	5.9 ± 5.8
Q_{yy}	-12.05 ± 3.1	-10.25^c		17.0 ± 4.5	-9.7 ± 4.5
Q_{zz}	$+24.1 \pm 3.1$	20.5^c		29.5 ± 5.6	3.8 ± 5.2
χ^P_{xx}	147.9 ± 1.0	245.9^c		156.9 ± 1.4	227.4 ± 0.6
χ^P_{yy}	147.9 ± 1.0	245.9^c		125.0 ± 1.8	226.4 ± 0.9
χ^P_{zz}	259.6 ± 1.0	251.4^c		251.0 ± 1.7	221.6 ± 3.1
$\langle y^2 \rangle - \langle x^2 \rangle$	0	0		7.7 ± 0.8	0.8 ± 1.0
$\langle z^2 \rangle - \langle x^2 \rangle$	-26.6 ± 0.3	-1.7^c		-22.0 ± 0.8	-0.2 ± 1.0

[a] The magnetic susceptibilities are in units of 10^{-6} erg/G^2 mol, the units on the molecular quadrupole moments are 10^{-26} esu cm^2, and the units of $\langle y^2 \rangle$ are 10^{-16} cm^2. [b] $|g_{||}| = 0.0815$ in OPF_3 is assumed to be equal to the corresponding experimental $g_{||}$ in PF_3. [c] Follows from assumption in footnote b. [d] The g values in NF_3 are negative from the measurement.
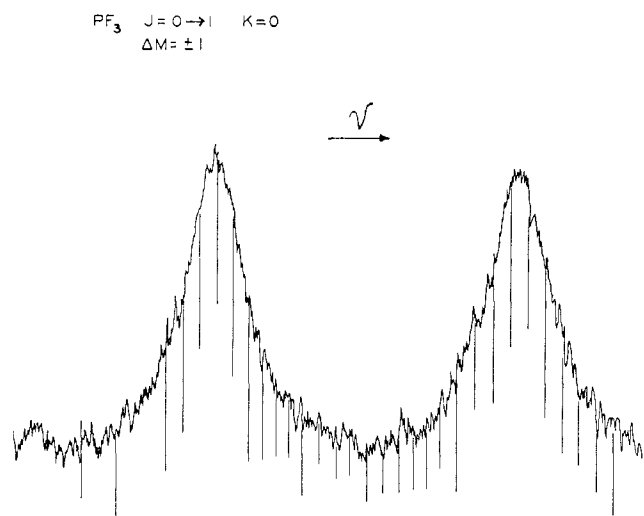

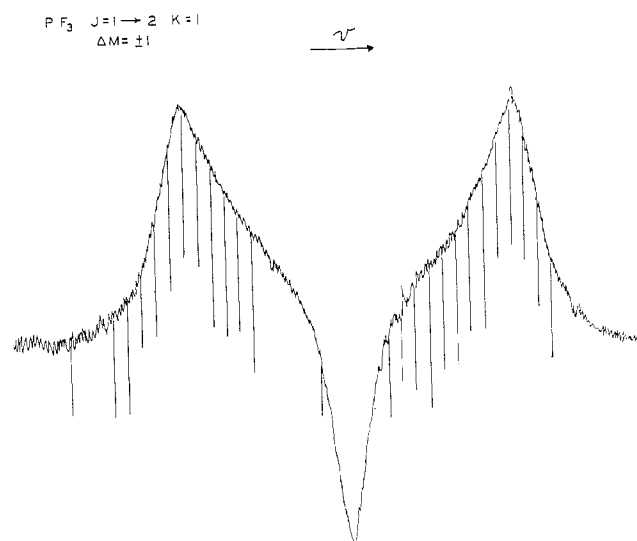Figure 2.—A trace of the $J = 0 \to 1$, $\Delta M = \pm 1$, $K = 0$ spectrum in PF_3 at 25,386 G. The markers are every 100 kHz.

Figure 3.—The $J = 1 \to 2$, $\Delta M = \pm 1$, $K = 1$ transition in PF_3 at 25,055 G. The markers are every 100 kHz.

positive (eq 20). This gives the most probable sign of the g values as negative.

The most probable results for $g_\perp$ and $g_{||}$ both negative are listed in Table III.

The diagonal elements in the paramagnetic susceptibility tensor are directly obtained from the negative g values and the molecular structure shown in Figure 1. Using eq 12 gives (in units of 10^{-6} erg/G^2 mol) the following values. The results for positive g values are in parentheses.

$$\chi^P_\perp = 147.9 \pm 1.0 \ (112.1)$$
$$\chi^P_{||} = 259.6 \pm 1.0 \ (183.8) \tag{22}$$

The anisotropy in the electronic charge distribution is also easily obtained from eq 11 and the result is shown in Table III.

The bulk susceptibility has apparently not been measured in PF_3. However, we can estimate χ in PF_3 from the known value of $\chi = -63.2 \times 10^{-6}$ erg/G^2 mol in PCl_3[13] and Pascal's rules.[14] The method is to estimate χ in PF_3 by subtracting the difference

between the Pascal atomic contributions in Cl and F. Thus, according to Pascal's rules

$$\chi(PF_3) = \chi_P + 3\chi_F$$
$$\chi(PCl_3) = \chi_P + 3\chi_{Cl}$$

Thus

$$\chi(PCl_3) = \chi(PF_3) - 3(\chi_{Cl} - \chi_F)$$

The value of $(\chi_{Cl} - \chi_F)$ is taken from Selwood's table. Other tables[15] give different values for $(\chi_{Cl} - \chi_F)$. However, Selwood's work seems to correlate best with the known inorganic compounds such as SCl_2, SCl_3, $SOCl_2$, SO_2Cl_2, SH_2, SO_2, $COCl_2$, SeO_3, $CSCl_2$, $CHBr_3$, $CHCl_3$, PBr_3, $POBr_3$, PCl_3, and $POCl_3$.[16] In any event, using $(\chi_{Cl} - \chi_F) = -8.6 \times 10^{-6}$ erg/G^2 mol from Selwood gives the estimated value for PF_3

$$\chi(PF_3) = -37.4 \times 10^{-6} \text{ erg/}G^2 \text{ mol}$$

(13) P. Pascal, *Compt. Rend.*, **218**, 57 (1944).
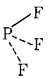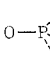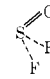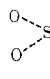
(14) P. W. Selwood, "Magnetochemistry," Interscience Publishers, New York, N. Y., 1943.

(15) P. Pascal, "Chimie generale," Masson et Cie, Paris, 1949. These constants seem to be the most widely used. See, for instance, J. A. Pople, W. G. Schneider, and H. J. Bernstein, "High-Resolution Nuclear Magnetic Resonance," McGraw-Hill Book Co., Inc., New York, N. Y., 1959.

(16) Landolt-Börnstein, "Physikalish-chemishe Tabellen," Vol. 2, Springer-Verlag, Berlin, 1951, Part 10.

Taking the value of -37.4×10^{-6} erg/G^2 mol calculated for the bulk susceptibility of PF_3, the diagonal elements of the paramagnetic and diamagnetic tensor and the second moment charge distribution of the molecule can be calculated using eq 11–13. The susceptibility results obtained for the negative set of g values are (all in units of erg/G^2 mol)

$$\chi_\perp = -36.9 \times 10^{-6}$$
$$\chi_{||} = -38.3 \times 10^{-6}$$
$$\chi^d_\perp = -184.9 \times 10^{-6}$$
$$\chi^d_{||} = -297.9 \times 10^{-6}$$

(23)

These results are summarized in Table IV. As these numbers are estimates based above on χ, no uncertainties are listed.

TABLE IV

THE MAGNETIC SUSCEPTIBILITY TENSOR ELEMENTS COMPUTED FROM ESTIMATED VALUES FOR χ (SEE TEXT), EQ 13 AND 14, AND THE EXPERIMENTAL PARAMETERS IN TABLE II[a]

	$\begin{array}{c} _{F} \\ P{-}F \\ F \end{array}$	$\begin{array}{c} _{F} \\ O{-}P{-}F \\ F \end{array}$	$\begin{array}{c} O \\ S{-}F \\ F \end{array}$	$\begin{array}{c} O _{F} \\ S \\ O _{F} \end{array}$
$\chi = \frac{1}{3}(\chi_{xx} + \chi_{yy} + \chi_{zz})$	-37.4	-42.0	-27.1	-36.9
χ_{xx}	-36.9	-43.2	-27.6	-37.1
χ_{yy}	-36.9	-43.2	-26.9	-32.5
χ_{zz}	-38.3	-41.6	-26.9	-41.4
χ^d_{xx}	-184.9	-287.4	-184.5	-263.5
χ^d_{yy}	-184.9	-287.4	-151.9	-260.0
χ^d_{zz}	-297.9	-294.7	-277.9	-262.7
$\langle x^2 \rangle$	35.1	34.7	28.9	30.5
$\langle y^2 \rangle$	35.1	34.7	36.6	31.4
$\langle z^2 \rangle$	8.5	33.0	6.9	30.7

[a] As all numbers are estimates from our assumed values of χ, no uncertainties are listed. The units of the susceptibilities are 10^{-6} erg/G^2 mol and the units on $\langle x^2 \rangle$ are 10^{-16} cm^2.

The resulting center of mass average values of $\langle a^2 \rangle$ and $\langle b^2 \rangle$ over all molecular electrons are listed below and in Table IV.

$$\langle 0 | \sum_i a_i^2 | 0 \rangle = 8.47 \times 10^{-16} \text{ cm}^2$$

$$\langle 0 | \sum_i b_i^2 | 0 \rangle = \langle 0 | \sum_i c_i^2 | 0 \rangle = 35.09 \times 10^{-16} \text{ cm}^2$$

POF$_3$.—The $J = 0 \to 1$, $\Delta M = \pm 1$ doublet was observed several times at a magnetic field of 25,216 G. An average splitting of 1692 ± 15 kHz was found. With the use of eq 7, the absolute value of $g_\perp$ is found to be

$$|g_\perp| = 0.0440 \pm 0.0005 \tag{24}$$

The average of the two peaks did not shift appreciably from the field off $J = 0 \to 1$ transition. Therefore, the $J = 0 \to 1$, $\Delta M = 0$ transition was observed to obtain $\chi_\perp - \chi_{||}$. As can be seen from eq 7 the shift of the transition will be twice as great with the $\Delta M = 0$ transition than the $\Delta M = \pm 1$ transitions. This shift was found to be 50 ± 5 kHz at 29,150 G and gives

$$\chi_\perp - \chi_{||} = (1.78 \pm 0.18) \times 10^{-6} \text{ erg/}G^2 \text{ mol} \tag{25}$$

The $K = 1$, $J = 1 \to 2$, $\Delta M = \pm 1$ transitions (see Table I) were observed in order to obtain the value of $g_{||}$. However, the splitting between the most intense transitions was sufficiently small that the presence of the very large Stark component near the zero-field frequency, ν_0, made the data collection unreliable. At 25,200 G we observed a doublet similar to the one shown in Figure 3. The Stark perturbation was much more severe owing to broader lines and we can only list an upper limit of 2 MHz for the splitting. The Stark effect interference can be seen in Figure 3, in the $K = 1$, $J = 1 \to 2$ transition of PF$_3$. Shoemaker and Flygare[6] have explained the presence of this anomalous Stark effect. The magnetic field for the $K = 1$ transition shown in

Figure 3 is perpendicular to the electric vector of the microwaves giving $\Delta M = \pm 1$ selection rules. The electric field used for Stark modulation is parallel to the microwave electric vector. A secular equation involving both the electric and magnetic fields must be solved for the energy levels. It is found that the $J = 1$, $M_J = 0$ and the $J = 2$, $M_J = 0$ levels are unchanged to first order by an electric and magnetic field. It is the transition between these two levels that appears near ν_0 when the electric field is strong enough to give appreciable $\Delta M = 0$ transition intensity.

Thus, we were unable to attain $g_{||}$ for POF$_3$ from the $K = 1$ spectra. However, the structure of the PF$_3$ part of the OPF$_3$ molecule is remarkably similar to the corresponding structure of the PF$_3$ molecule (see Figure 1). Therefore, we would expect $g_{||}$ in OPF$_3$ to be nearly identical with the value in PF$_3$. The values of $g_{||}$ in $CH_3C{\equiv}CH$, H_3CI, H_3CBr, and CH_4 are also nearly identical.[6] Thus, using $|g_{||}| = 0.0815$ for OPF$_3$ we can compute the molecular quadrupole moments. The results are given in eq 26 and 27 for both choices in signs for the $g_\perp$ in eq 24. The units are 10^{-26} esu cm^2. The value of 20.5 appears more

$$g_\perp = 0.0440 \pm 0.0005, \, g_{||} = 0.0815$$

$$Q_{||} = -16.4 \tag{26}$$

$$g_\perp = -0.0440 \pm 0.0005, \, g_{||} = -0.0815$$

$$Q_{||} = -20.5 \tag{27}$$

reasonable which assigns the signs of the g values as negative.

We can now compute the predicted spectra for the $J = 1 \to 2$, $\Delta M = \pm 1$, $K = 1$ transition with $g_\perp = \pm 0.0440$ and $g_{||} = \pm 0.0815$ to find if the predicted spectrum contradicts our observed broad doublet with an upper limit for the splitting of 2 MHz as quoted above. The calculated spectrum is listed in Table V. This spectrum predicts a splitting of about 1.8–2.0 MHz which is consistent with our observed spectra.

TABLE V

CALCULATED $\Delta M = \pm 1$ TRANSITION SPLITTINGS FROM ν_0 (IN kHz) IN THE $J = 1 \to J = 2$, $K = 1$ TRANSITION IN OPF$_3$ AT A FIELD OF 25,200 G AS DISCUSSED IN THE TEXT[a]

$J = 1 \to J = 2$ $M \to M$	Rel intens	$\Delta \nu$	$J = 2$ $M \to M$	Rel intens	$\Delta \nu$
$-1 \to 0$	2	-1207 (1207)	$-1 \to -2$	12	699 (-459)
$0 \to 1$	6	-936 (1004)	$0 \to -1$	6	1000 (-936)
$1 \to 2$	12	-459 (699)	$1 \to 0$	2	1217 (-1207)

[a] The results are given for $g_\perp = 0.0440$ and $g_{||} = 0.0815$ as discussed in the test. Splittings for the negative g values are in parentheses.

Using the molecular structure in Figure 1 and the Zeeman parameters above with eq 12 yields the diagonal elements in the paramagnetic susceptibility tensor as also shown in Table III.

The bulk susceptibility for POF$_3$ was calculated from the known value in OPCl$_3$ ($\chi = -67.8 \times 10^{-6}$ erg/G^2 mol)[17] in the manner previously described using $\chi_{Cl} - \chi_F = -8.6 \times 10^{-6}$ erg/G^2 mol as discussed previously. The resultant bulk susceptibility for OPF$_3$ is

$$\chi = -42.0 \times 10^{-6} \text{ erg/}G^2 \text{ mol} \tag{28}$$

Using this value, the diagonal elements of the total and diamagnetic susceptibility tensor elements were calculated. The results are listed in Table IV. Also listed are the individual elements in the second moment of the electronic charge distribution (Table IV).

^{14}NF$_3$.—The ^{14}NF$_3$ Zeeman spectrum is considerably more complex than the other symmetric tops studied here (PF$_3$ and OPF$_3$) owing to the presence of the ^{14}N nuclear quadrupole coupling. The ^{14}NF$_3$ case considered here is identical in form

(17) M. W. Lister and R. Marson, *Can. J. Chem.*, **42**, 1817 (1964).

with the $H_3CC^{14}N$ Zeeman spectrum which is discussed in detail by Pochan, Stone, and Flygare.[18] The first-order Zeeman energy in the uncoupled basis is given as

$$E(J,K,M_J,I,M_I) = -\mu_0 H\Bigg[M_I g_I +$$

$$M_J\Big(g_\perp + \frac{K^2}{J(J+1)}(g_{||} - g_\perp)\Big) - \frac{hX^N}{2} \times$$

$$\Big(1 - \frac{3K^2}{J(J+1)}\Big)\Big(\frac{1}{2I(2I-1)(2J-1)(2J+3)}\Big) \times$$

$$(J(J+1) - 3M_J{}^2)(I(I+1) - 3M_I{}^2) -$$

$$\frac{H^2}{3}\Big[\frac{3M_J{}^2 - J(J+1)}{(2J-1)(2J+3)}\Big]\Big[(\chi_\perp - \chi_{||}) -$$

$$\frac{3K^2}{J(J+1)}(\chi_\perp - \chi_{||})\Bigg] \quad (29)$$

X^N is the ^{14}N nuclear quadrupole coupling constant along the C_3 axis, μ_0 is the nuclear magneton as before, I and M_I are the nuclear quantum numbers, and g_I is the nuclear g value. If the angular momenta of the system are not completely decoupled by the applied magnetic field, off-diagonal elements in M_J and M_I that are functions of the nuclear quadrupole coupling constant must be incorporated into the molecular energy scheme.[18]

The complete matrix description of the $J = 1$ state in the intermediate coupling region has been described before[18] and the energy levels are easily obtained as a function of $g_\perp$, $g_{||}$, g_N, X^N, and $(\chi_\perp - \chi_{||})$. In the intermediate case, all of the states considered in the absence of nuclear coupling are tripled due to the $M_I = 0$ and ± 1 states. Thus, the $J = 0 \rightarrow J = 1$, $\Delta M_J = \pm 1$ transition in the $^{14}NF_3$ Zeeman spectrum appeared as a six-line spectrum with the assignment shown in Table VI. The six-

TABLE VI
THE OBSERVED AND CALCULATED $J = 0 \rightarrow 1$, $\Delta M_J = \pm 1$,
$\Delta M_I = 0$ SPECTRA IN $^{14}NF_3{}^a$

	M_J(lower) →	$\Delta\nu$		
M_I	M_J(upper)	Obsd	Calcd	Diff
1	$0 \rightarrow -1$	-1.108	-1.103	-0.005
1	$0 \rightarrow 1$	1.548	1.549	-0.004
0	$0 \rightarrow -1$	-1.951	-1.957	0.006
0	$0 \rightarrow 1$	0.599	0.604	-0.005
-1	$0 \rightarrow -1$	-0.785	-0.770	-0.015
-1	$0 \rightarrow 1$	1.947	1.956	-0.009

^{a} Six lines were resolved and assigned as shown. The frequencies are listed in MHz from ν_0.

line high-field $J = 0 \rightarrow J = 1$ spectra in NF_3 should be compared to the doublet spectrum shown for PF_3 in Figure 2 (in the absence of nuclear coupling). The six-line $^{14}N_3$ $\Delta M = \pm 1$, $K = 0$, $J = 0 \rightarrow J = 1$ spectrum described in Table VI was interpreted with a matrix diagonalization of the $J = 1$ state (9×9 matrix) as described above and in our previous work for the intermediate coupling region.[18]

The value of X^N or the ^{14}N nuclear quadrupole coupling constant obtained from the zero-field spectrum is also needed as input in the above matrix diagonalization. We have observed this zero-field triplet and our value of $X^N(^{14}N) = -7.067 \pm 0.018$ MHz agrees very well with the previously measured value.[19]

(18) J. M. Pochan, R. G. Stone, and W. H. Flygare, *J. Chem. Phys.*, in press.
(19) C. H. Townes and A. L. Schawlow, "Microwave Spectroscopy," McGraw-Hill Book Co., Inc., New York, N. Y., 1955.

The resultant analysis of the high-field $J = 0 \rightarrow J = 1$ transition in $^{14}NF_3$ at 25,301 G gave the Zeeman parameters

$$g_\perp = -0.060 \pm 0.001$$
$$\chi_\perp - \chi_{||} = -(3.0 \pm 1.5) \times 10^{-6} \text{ erg/G}^2 \text{ mol} \quad (30)$$

The sign of $g_\perp$ is obtained from this analysis due to the reference to the known sign of the ^{14}N nuclear g value. The values for the calculated splittings in Table VI are from eq 30 and $X^N(^{14}N) = -7.067 \pm 0.018$ Hz as measured in this work.

We could not measure $g_{||}$ in this work as the $J = 1 \rightarrow J = 2$ transition in $^{14}NF_3$ lies above our available frequency range (40.0 GHz). Therefore, no further analysis on NF_3 will be given at this time.

SOF₂.—The $0_{00} \rightarrow 1_{10}$, and $1_{01} \rightarrow 2_{11}$ $\Delta M = 0$ and $\Delta M = \pm 1$ transitions were measured, along with the $1_{11} \rightarrow 2_{21}$ $\Delta M = \pm 1$ transition. The data, which are listed in Table VII, were then

TABLE VII
THE OBSERVED AND CALCULATED TRANSITIONS AND ZEEMAN
SPLITTINGS IN SOF₂

Transition	$M \rightarrow M'$	ν_0, MHz	Obsd	Calcd	H, G
$0_{00} \rightarrow 1_{10}$		16,971.80			25,420
$\Delta M = \pm 1$	$0 \rightarrow -1$		$+1506$	$+1611$	
	$0 \rightarrow +1$		-1510	-1602	
$\Delta M = 0$	$0 \rightarrow 0$		-25	-10	28,119
$1_{11} \rightarrow 2_{21}$		34,201.10			25,170
$\Delta M = \pm 1$	$-1 \rightarrow -2$		$+1520$	$+1483$	
	$+1 \rightarrow +2$		-1606	-1478	
$1_{01} \rightarrow 2_{11}$		33,685.48			25,125
$\Delta M = \pm 1$	$-1 \rightarrow -2$		$+1640$	$+1537$	
	$+1 \rightarrow +2$		-1470	-1522	
$\Delta M = 0$	$+1 \rightarrow +1$		$+188$	$+183$	29,020
	$0 \rightarrow 0$		$+4$	-5	
	$-1 \rightarrow -1$		-205	-207	

fit with a least-squares computer program[2,4,5] to give the g values and the magnetic susceptibility anisotropies along the principal inertial axes. The g values are $|g_{aa}| = 0.0802 \pm 0.0070$, $|g_{bb}| = 0.0856 \pm 0.0051$, and $|g_{cc}| = 0.1093 \pm 0.0038$. All g values have the same sign. The magnetic susceptibility anisotropies are $2\chi_{aa} - \chi_{bb} - \chi_{cc} = (0.67 \pm 1.60) \times 10^{-6}$ erg/G² mol and $2\chi_{bb} - \chi_{cc} - \chi_{aa} = -(1.46 \pm 2.09) \times 10^{-6}$ erg/G² mol. Predicted spectra using the above parameters are also listed in Table VII. The Zeeman parameters are also listed in Table III.

The molecular quadrupole moments were calculated using both positive and negative g values and eq 8. The results are given in eq 31 and 32.

positive g values

$$Q_{aa} = +16.3 \pm 4.5$$
$$Q_{bb} = +14.1 \pm 4.5 \quad (31)$$
$$Q_{cc} = -30.4 \pm 5.6$$

negative g values

$$Q_{aa} = -17.0 \pm 4.5$$
$$Q_{bb} = -12.5 \pm 4.5 \quad (32)$$
$$Q_{cc} = +29.5 \pm 5.6$$

As SOF_2 is isoelectronic with PF_3, we would expect the c axis in SOF_2 to approximate the C_3 axis in PF_3. On this basis we prefer the molecular quadrupole moments in eq 32 in SOF_2 by comparison with PF_3 (see Figure 1 and Table III). The similarity between the corresponding molecular quadrupole moments in PF_3 and SOF_2 is quite striking.

Using the molecular structure in Figure 1 and the molecular g values in Table III for SOF_2 allows a determination of the diagonal elements in the paramagnetic susceptibility tensor (see eq 12). The results are listed in Table IV. The anisotropies in the second moment of the electronic charge distribution are also listed in Table IV (see eq 11).

Taking the negative g values and a bulk susceptibility of -27.1×10^{-6} erg/G^2 mol calculated using Pascal's rules and the bulk susceptibility of $SOCl_2$ (-44.3×10^{-6} erg/G^2 mol),[20] the diagonal elements of the total and diamagnetic susceptibility tensors and the individual second moments of the electron distribution were calculated. The results are listed in Table IV.

SO_2F_2.—Two $1 \rightarrow 2$ $\Delta M = \pm 1$ and two $2 \rightarrow 3$ $\Delta M = 0$ and $\Delta M = \pm 1$ transitions were measured in SO_2F_2. The results are listed in Table VIII. All of the $\Delta M = \pm 1$ transitions were observed to be doublets, the individual M components not being resolved. In all of these transitions, the frequencies of the doublets were assumed to be those of the strongest M transitions. In the

TABLE VIII
THE OBSERVED AND CALCULATED TRANSITIONS AND ZEEMAN SPLITTINGS IN SO_2F_2

Transition $M \rightarrow M'$	ν_0, MHz	Obsd	Calcd	H, G
$1_{01} \rightarrow 2_{02}$	29,257.48			
$\Delta M = \pm 1$ $\quad -1 \rightarrow -2$		$+1008$	$+998$	25,247
$\quad\quad\quad +1 \rightarrow +2$		-1008	-1021	
$1_{10} \rightarrow 2_{11}$	20,276.25			
$\Delta M = \pm 1$ $\quad -1 \rightarrow -2$		$+811$	$+856$	25,341
$\quad\quad\quad +1 \rightarrow +2$		-1080	-1051	
$2_{11} \rightarrow 3_{12}$	30,412.41			
$\Delta M = \pm 1$ $\quad -2 \rightarrow -3$		$+927$	$+917$	25,205
$\quad\quad\quad +2 \rightarrow +3$		-978	-990	
$2_{12} \rightarrow 3_{13}$	30,364.64			
$\Delta M = \pm 1$ $\quad -2 \rightarrow -3$		$+1063$	$+1029$	25,118
$\quad\quad\quad +2 \rightarrow +3$		-1055	-1072	
$\Delta M = 0$ $\quad -1 \rightarrow -1$			$+32$	29,084
$\quad\quad\quad 0 \rightarrow 0$		$+27$	$+24$	
$\quad\quad\quad +1 \rightarrow +1$			$+1$	
$2_{02} \rightarrow 3_{03}$	30,379.82			
$\Delta M = \pm 1$ $\quad -2 \rightarrow -3$		$+1033$	$+1059$	25,259
$\quad\quad\quad +2 \rightarrow +3$		-1034	-1035	
$\Delta M = 0$ $\quad -1 \rightarrow -1$			$+21$	29,120
$\quad\quad\quad 0 \rightarrow 0$		$+8$	-33	
$\quad\quad\quad +1 \rightarrow +1$			-18	

$\Delta M = 0$ transitions, no splittings were obtained and the peaks were only observed to broaden and shift slightly when the magnetic field was turned on. The data (see Table VIII) were used to obtain the g values and magnetic susceptibility anisotropies by fitting them with a least-squares program. The g values which were obtained are

$$|g_{aa}| = 0.0447 \pm 0.0068$$
$$|g_{bb}| = 0.0456 \pm 0.0015 \qquad (33)$$
$$|g_{cc}| = 0.0565 \pm 0.0009$$

All g values are of the same sign. The magnetic susceptibility anisotropies are $2\chi_{aa} - \chi_{bb} - \chi_{cc} = -(12.6 \pm 2.6) \times 10^{-6}$ erg/G^2 mol and $2\chi_{bb} - \chi_{cc} - \chi_{aa} = (13.2 \pm 3.5) \times 10^{-6}$ erg/G^2 mol.

The molecular quadrupole moments were calculated using both positive and negative g values. The results are given in eq 34 and 35.

g values positive

$$Q_{aa} = 10.4 \pm 5.2$$
$$Q_{bb} = -5.2 \pm 4.5 \qquad (34)$$
$$Q_{cc} = -5.2 \pm 5.8$$

g values negative

$$Q_{aa} = +3.8 \pm 5.2$$
$$Q_{bb} = -9.7 \pm 4.5 \qquad (35)$$
$$Q_{cc} = +5.9 \pm 5.8$$

When one considers the relationship of the inertial axes to the molecular structure (see Figure 1) and the quadrupole moments along these axes, the moments obtained with all g values negative seem more reasonable. The b and c axes are in SF_2 and SO_2 planes, respectively, and should have similar quadrupole moments, while the moment along the a axis should be considerably different. Thus, we favor the negative g values as in PF_3, OPF_3, and SOF_2.

Using the molecular structure listed in Figure 1 for SO_2F_2, the negative g values, and eq 11 and 12 gives the remaining results in Table III.

The bulk magnetic susceptibility in SO_2Cl_2 is $\chi = -62.7 \times 10^{-6}$ erg/G^2 mol.[21] Using this number and Pascal's rules as before allows an estimate for SO_2F_2 which is $\chi = -36.9 \times 10^{-6}$ erg/G^2 mol. The remaining numbers in Table IV follow from this estimate.

IV. Discussion

The quadrupole moments and molecular structures for the series of inorganic molecules studied here are listed in Figure 1. Except for SO_2F_2 all of these molecules have large positive quadrupole moments along their symmetry axes. In the case of SOF_2 this would correspond to the c axis. PF_3 has three highly electronegative fluorine atoms in a prolate structure giving the large positive quadrupole moment. In POF_3 the oxygen atom has the effect of making that end of the molecule more negative which appears in the size of Q_{aa}. In SOF_2 we have no true symmetry axis but the c inertial axis is closest to the corresponding symmetry axes in PF_3 and POF_3. Again the large positive quadrupole moment is evident.

In SO_2F_2 the quadrupole moment along the symmetry axis is small and positive. The most remarkable feature in this molecule is best illustrated in the second moments of the electron distribution along the inertial axes. These most definitely show that the electron distribution in this molecule is nearly spherical.

In NF_3 the molecular g value is measured to be negative by reference to the sign of the ^{14}N nuclear magnetic moment. This lends further support to the assignment of negative g values to all of the other molecules studied here. Furthermore, a recent reliable calculation of $Q_{||}$ in NF_3 gives $Q_{||} = +6.12$.[22] Thus, the positive value of $Q_{||}$ in NF_3 lends support again for the positive values of $Q_{||}$ in PF_3 and SOF_2 and the negative signs for the g values.

(20) P. S. Varadachari and K. C. Subramaniam, *Proc. Indian Acad. Sci.*, A, **3**, 428 (1936).

(21) K. Kido, *Sci. Rept. Tohoku Univ.*, **21**, 869 (1932).
(22) M. L. Unland, J. H. Letcher, and J. R. Van Wazer, *J. Chem. Phys.*, **50**, 3214 (1969).

All of the molecules studied here have remarkably small magnetic susceptibility anisotropies compared to the large values reported for ring compounds.[3-5] As the values reported in Table IV are all computed from an estimated bulk susceptibility, they deserve further comment. In Table IV the values of $\langle x^2 \rangle$ in PF_3, OPF_3, and SOF_2 should be within 10% of each other.

The value of $\langle x^2 \rangle$ in SOF_2 is anomalously low which indicates that the Pascal value of χ in SOF_2 is too small. The remaining numbers would fall into approximate order if the magnitude of χ in SOF_2 were larger.

Contribution from the Department of Chemistry,
Rice University, Houston, Texas 77001

Silicon–Fluorine Chemistry. VII.
The Reaction of Silicon Difluoride with Hydrogen Sulfide

By KENNETH G. SHARP and J. L. MARGRAVE

A study of the reaction of silicon difluoride with hydrogen sulfide by cocondensing the reactants at liquid nitrogen temperature has been made. The resultant low-temperature polymer yielded the following compounds as it warmed to room temperature: SiF_2HSH, SiF_2HSiF_2SH, Si_2F_5H, and small amounts of SiF_2HSSH and Si_2F_4HSSH. These compounds could also be obtained by pyrolysis of the polymer at 120–140°. SiF_2HSH was observed to react with HCl to form SiF_2HCl and H_2S. Compounds were characterized by means of mass spectrometry and, where possible, by ^1H and ^{19}F nmr and by infrared spectroscopy.

Introduction

The divalent carbene-like molecule silicon difluoride has been shown to possess an extensive reaction chemistry at low temperatures.[1-3] SiF_2 is customarily generated at high temperatures then cocondensed at $-196°$ with a particular reactant. Reaction occurs as the condensate is allowed to warm to room temperature. A portion of the reaction products can generally be recovered as volatile products—the rest are bound in an involatile polymer which may often be pyrolyzed as a further source of products.

Much of the reaction chemistry of SiF_2 may be explained on the assumption that the reactive species are diradicals $\cdot SiF_2(SiF_2)_nSiF_2\cdot$ where $n = 0, 1, 2$, etc. The $n = 0$ species is the most favorable kinetically for addition reactions of the type $AB + (SiF_2)_{n+2} = SiF_2A(SiF_2)_nSiF_2B$, and in such reactions the predominant product often contains two silicon atoms.[1-3]

Solan and Timms[4] have recently reported the reaction of SiF_2 with GeH_4. The products obtained correspond to the formula $GeH_3(SiF_2)_nH$, with $n = 1–3$. The $n = 1$ homolog was the major product and was the only one of the products which was stable at room temperature. The authors suggested that the "usual" diradical dimer mechanism was not operative in this instance and that GeH_4 attacks the SiF_2 polymeric chain, breaking off units containing one, two, or more silicon atoms.

The H_2S reaction might be expected to follow several different courses. If, for example, reaction occurs exclusively with the SiF_2 dimer, the logical product would be SiF_2HSiF_2SH. H_2S is known to add across double bonds in the presence of radical initiators.[5] If the reaction were to proceed in a manner similar to that of the germane reaction, one would expect the products SiF_2HSH, SiF_2HSiF_2SH, and so on. In addition, previous reactions of SiF_2 with dimethyl ether, acetonitrile, and acetone[6] have indicated that SiF_2 is capable of abstracting a hydrogen atom from such molecules to form eventually SiF_3H, so that such a course would not be surprising for the H_2S reaction.

Few silanethiols, such as the products mentioned above, are known. The literature contains references to SiH_3SH,[7] $SiCl_3SH$,[8] and $(C_2H_5)_3SiSH$,[9] and few others. The parent compound silanethiol was synthesized by Eméleus, *et al.*, from the reaction of disilyl sulfide with hydrogen sulfide and was found to be unstable with respect to condensation back into starting materials, even at temperatures as low as $-78°$. Such compounds as SiF_3SH or SiF_2HSH should be more stable than silanethiol itself because the electron-withdrawing power of the fluorines would make the Si–S bond more polar.

(1) P. L. Timms, T. C. Ehlert, J. L. Margrave, F. E. Brinckman, T. C. Farrar, and T. D. Coyle, *J. Am. Chem. Soc.*, **87**, 3819 (1965).

(2) P. L. Timms, D. D. Stump, R. A. Kent, and J. L. Margrave, *ibid.*, **88**, 940 (1966).

(3) J. C. Thompson, J. L. Margrave, and P. L. Timms, *Chem. Commun.*, 566 (1966).

(4) D. Solan and P. L. Timms, *Inorg. Chem.*, **7**, 2157 (1968).

(5) R. E. Foster, A. W. Larchar, R. D. Lipscomb, and B. C. McKusick, *J. Am. Chem. Soc.*, **78**, 5606 (1956).

(6) K. G. Sharp, Ph.D. Thesis, Rice University, 1969.

(7) H. J. Eméleus, A. G. MacDiarmid, and A. G. Maddock, *J. Inorg Nucl. Chem.*, **1**, 194 (1955).

(8) W. C. Schumb and W. J. Bernard, *J. Am. Chem. Soc.*, **77**, 862 (1955).

(9) E. Larsson and R. Marin, *Acta Chem. Scand.*, **5**, 964 (1951).